Beamforming mmWave MIMO: Impact of Nonideal Hardware and Channel State Information

Nebojsa Maletic, *Member, IEEE*, Jesús Gutiérrez-Teran, and Eckhard Grass

Abstract—In this paper, we analyzed the impact of residual hardware impairments on the performance of different beamforming millimeter wave (mmWave) Multiple-Input Multiple-Output (MIMO) architectures. By modeling the residual impairments as a additional distortion noise, expression for the capacity for both hybrid beamforming and analog RF beamforming mmWave MIMO is obtained. For the analog RF beamforming, an analytical upper bound is derived. Additionally, the effect of nonideal channel state information is investigated. Performance of the beamforming mmWave MIMO are assessed through Monte Carlo simulations. Results confirm that hardware impairments are limiting the systems performance.

Keywords—Beamforming, mmWave, MIMO, impairments.

I. INTRODUCTION

Millimeter wave (mmWave)-based wireless communication systems are seen as a key technology enablers for the fifth generation (5G) systems deployment [1]. High data rates are achievable due to large amount of wide bandwidths available in the mmWave spectrum. In addition, small wavelength allows deployment of large antenna arrays which can be packed in small-form factor. This way mmWave systems can achieve sufficient power combining and beamforming gain to combat with the high free-space path loss of mmWave signals and to provide sufficient link budget [2], [3].

With the large antenna arrays integration of mmWave and MIMO in conventional way, where each antenna has dedicated radio-frequency (RF) chain, would be unfeasible. Conventional MIMO would introduce high hardware costs and energy consumption at mmWave frequencies. One solution to reduce the number of RF chains is to use analog RF beamforming [4]. Here, signal processing is performed in RF domain using network of phase shifters. This solution can support only single stream transmission [4]. For example, analog beamforming mmWave MIMO is used in IEEE 802.11ad standard [5]. To achieve higher spectral efficiencies and multi-stream support, a hybrid beamforming solution for MIMO at mmWave is proposed [6]-[11]. This solution is a compromise between all-digital beamforming (precoding)[1] and analog RF beamforming. It has small-size digital precoder and large-size analog RF beamformer. Depending on the structure of the analog RF beamformer, fully-connected and partially-connected structures are possible. In the former signal at the output of each RF chain is connected to all antennas through the network of phase shifters, while in the latter each RF chain is connected to antenna subset [12]. Due to digital precoder, small number of RF chains (typically 2-4) is possible. Most of the research work is focused on the precoder design and its complexity reduction [12]-[15], transceiver design for hybrid beamforming [16], beam training and RF codebook design [17] and channel estimation using compressive sensing tools [18]. Although shown that hybrid beamforming mmWave MIMO systems can achieve increased spectral efficiency and performance very close to its digital counterpart, numerous works on the hybrid beamforming assume ideal hardware. Practical systems have nonideal hardware which introduces impairments, thus affecting their performance.

In this paper, we analyze the performance of beamforming mmWave MIMO from the system perspective considering nonideal hardware. The residual hardware impairment is modeled as a additional distortion noise, and then added to the system model. In addition, nonideal channel state information (CSI) is analyzed. For both hybrid and analog RF beamforming mmWave MIMO, we obtain the expressions for the capacity. For the latter one, we derive an analytical upper bound. Simulation results reveal that the distortion noise due to imperfect hardware has significant impact on the system performance introducing the ceiling effect.

This paper is organized as follows: Section II introduces system and channel model. Section III covers impairment model and performance analysis, while simulation results with the accompanying discussion is given in Section IV. Section V concludes the paper.

II. SYSTEM AND CHANNEL MODEL

A. System Model

We consider a single user hybrid precoding mmWave MIMO system, where N_s data streams are sent from a transmitter with N_t antennas to a receiver with N_r antennas. The transmitter and receiver have N_{RF}^t and N_{RF}^r radio-frequency (RF) chains, respectively, which are subject to the

[1]Often term *precoding* is used. Throughout this paper both beamforming and precoding will be used equally.
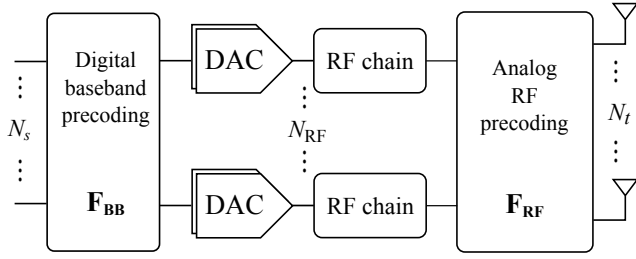
Fig. 1. Hybrid precoding transmitter architecture.

constraint $N_s \leq N_{RF}^x \leq N_x$, $x \in \{t, r\}$. Fig. 1 shows the corresponding transmitter architecture with hybrid precoding. The hybrid combiner architecture of the receiver would be straightforward. The transmitted signal vector can be written as $\mathbf{x} = \mathbf{F}_{RF}\mathbf{F}_{BB}\mathbf{s}$, where $\mathbf{s} \in \mathcal{C}^{N_s \times 1}$ is the symbol vector with $\mathbb{E}\left[\mathbf{s}\mathbf{s}^H\right] = \frac{1}{N_s}\mathbf{I}_{N_s}$. The hybrid precoder consists of a digital baseband precoder $\mathbf{F}_{BB} \in \mathcal{C}^{N_{RF}^t \times N_s}$, and an analog RF precoder $F_{RF} \in \mathcal{C}^{N_t \times N_{RF}^t}$. To meet the power constraint, we have $||\mathbf{F}_{RF}\mathbf{F}_{BB}||_F^2 = N_s$. The receiver uses the hybrid combiner $\mathbf{W}_H = \mathbf{W}_{BB}^H\mathbf{W}_{RF}^H$ and applies it to the received signal which, under perfect synchronization assumption, can be expressed as [6], [11]

$$\mathbf{y} = \sqrt{\rho}\mathbf{W}_{BB}^H\mathbf{W}_{RF}^H\mathbf{H}\mathbf{F}_{RF}\mathbf{F}_{BB}\mathbf{s} + \mathbf{W}_{BB}^H\mathbf{W}_{RF}^H\mathbf{n}, \quad (1)$$

where ρ is the average received power, $\mathbf{W}_{BB} \in \mathcal{C}^{N_{RF}^r \times N_s}$ is the digital baseband combiner, $W_{RF} \in \mathcal{C}^{N_r \times N_{RF}^r}$ is analog RF combiner, $\mathbf{H} \in \mathcal{C}^{N_r \times N_t}$ is the channel matrix with $\mathbb{E}\left[\mathbf{H}\mathbf{H}^H\right] = N_t N_r$, and $\mathbf{n} \in \mathcal{C}^{N_r \times 1}$ is the additive Gaussian noise vector with $\mathbb{E}\left[\mathbf{n}\mathbf{n}^H\right] = \sigma_n^2\mathbf{I}_{N_r}$. Assuming Gaussian distribution of the transmitted symbols, the capacity can be expressed as [6], [11]

$$R = \mathbb{E}\left\{\log_2\left|\mathbf{I}_{N_s} + \frac{SNR}{N_s}\left(\mathbf{W}_{RF}\mathbf{W}_{BB}\right)\mathbf{H}\mathbf{F}_{RF}\mathbf{F}_{BB}\right.\right.$$
$$\left.\left. \times \mathbf{F}_{BB}^H\mathbf{F}_{RF}^H\mathbf{H}^H\mathbf{W}_{RF}\mathbf{W}_{BB}\right|\right\}, \quad (2)$$

where $SNR = \rho/\sigma_n^2$.

To find optimal hybrid precoding/combining matrices, methods such as spatially sparse precoding (SS-P) [13], alternating minimization (AM) [11] for fully-connected analog structures and successive interference cancellation (SIC) hybrid precoding [12] for partially-connected analog structures can be used.

Note, when $N_s = N_{RF} = 1$, hybrid precoding collapses to analog RF precoding, for which the capacity is given by

$$R = \mathbb{E}\left\{\log_2\left(1 + SNR\left|\mathbf{w}^H\mathbf{H}\mathbf{f}\right|^2\right)\right\}, \quad (3)$$

where $\mathbf{w}$ is the beamcombining vector and $\mathbf{f}$ is the beamforming vector. This expression is maximized for $\mathbf{w} = \mathbf{U}(:,1)$ and $\mathbf{f} = \mathbf{V}(:,1)$, where $\mathbf{V}$ and $\mathbf{U}$ are the right and left singular vector matrices obtained after singular value decomposition (SVD) of the channel matrix $\mathbf{H} = \mathbf{U}\boldsymbol{\Lambda}\mathbf{V}^H$.

B. Channel Model

In this paper, as done in [11], [18], we adopt a narrowband, geometrical mmWave channel model expressed as

$$\mathbf{H} = \sqrt{\frac{N_T N_R}{L}}\sum_{l=0}^{L-1}\alpha_l\mathbf{a}_r(\theta_l^r, \phi_l^r)\mathbf{a}_t(\theta_l^t, \phi_l^t)^H, \quad (4)$$

where L represents the number of paths sourced from limited number of scatters, α_l is the complex gain of the l-th path, whereas $\phi_l^r(\theta_l^r)$ and $\phi_l^t(\theta_l^t)$ are the azimuth (elevation) angles of arrival and departure (AoD/AoAs), respectively. We assume that all α_l are independent and identically distributed (i.i.d.) random variables following $\mathcal{CN}(0, \sigma_i^2)$. In addition, $\mathbf{a}_t$ and $\mathbf{a}_r$ are the array response vectors at the transmitter and receiver, respectively.

For the uniform linear array (ULA) positioned on the y-axis ($\theta = \pi/2$) with N elements, the array response vector is given by [12]

$$\mathbf{a}(\phi) = \frac{1}{\sqrt{N}}\left[1, e^{j\frac{2\pi}{\lambda}d\sin(\phi)}, ..., e^{j(N-1)\frac{2\pi}{\lambda}d\sin(\phi)}\right]^T, \quad (5)$$

where λ denotes the wavelength of the signal and d is the antenna spacing. For the uniform planar array (UPA) positioned in the Oyz plane with N_h horizontal and N_v vertical antenna elements ($N = N_h N_v$), the array response vector is given by [12]

$$\mathbf{a}(\theta, \phi) = \frac{1}{\sqrt{N}}\left[1, ..., e^{j\frac{2\pi}{\lambda}d(p\sin(\phi)\sin(\theta)+q\cos(\theta))}, ...,\right.$$
$$\left. e^{j\frac{2\pi}{\lambda}d((N_h-1)\sin(\phi)\sin(\theta)+(N_v-1)\cos(\theta))}\right]^T, \quad (6)$$

where $0 \leq p \leq N_h - 1$ and $0 \leq q \leq N_v - 1$.

III. SYSTEM PERFORMANCE UNDER HARDWARE IMPAIRMENTS

In practical systems, RF transceivers introduce impairments which degrade their performance. These impairments originate from nonideal hardware components and are manifested as amplifier nonlinearity, phase noise, IQ-imbalance, DC offset, frequency offset, quantization noise, sampling jitter and so on [19]. Compensation schemes are often used to reduce the influence of the impairments, but some residual distortion remains. It is interesting to investigate how this residual distortion affects the performance of beamforming mmWave MIMO systems.

Owing to [20]-[22] the aggregate transceiver hardware impairments, which remain after compensation, can be approximated by independent additive distortion noises at both transmitter and receiver as

$$\boldsymbol{\Delta}_x \sim \mathcal{CN}(0, \kappa_x^2\boldsymbol{\Upsilon}_x), \quad x \in \{t, r\}, \quad (7)$$

where $\boldsymbol{\Upsilon}_x$ is the covariance matrix conditional on the channel, whereas κ_x represents proportionality parameter which describes the level of residual distortion noise at the transmitter or at the receiver. Furthermore, it is assumed that distortion noise is independent of the signal, but dependent on the channel realization and stationary only within the coherence time of

the channel. As stated in [20]-[22], the proportionality parameters are related to the error vector magnitude (EVM), which is a measure of RF transceiver quality. EVM requirements for the IEEE 802.11ad standard are in the range from -21 to -6 dB [5], which corresponds to $\kappa_x \in [0.089, 0.5]$. Clearly, smaller EVMs are needed to support higher modulation-coding schemes. $\kappa_x = 0$ reads ideal hardware.

According to [20] transmitter distortion is more dominant compared to the distortion at the receiver due to lower SNR at the reception. That is why, in this work, we consider only distortion at the transmitter side. Analysis that includes also receiver impairments is left for future work.

A. Hybrid precoding with residual Tx impairments

Owing to [21] the signal model including transmitter distortion noise at the passband can be expressed as

$$\mathbf{r} = \sqrt{\rho}\mathbf{H}_{\text{eff}}\mathbf{t} + \sqrt{\rho}\mathbf{H}_{\text{eff}}\boldsymbol{\Delta}_t + \mathbf{W}_{RF}^H\mathbf{n}, \quad (8)$$

where $\mathbf{H}_{\text{eff}} = \mathbf{W}_{RF}^H\mathbf{H}\mathbf{F}_{RF}$ is the effective channel seen at the passband after analog beamcombining, and $\mathbf{t} = \mathbf{F}_{BB}\mathbf{s}$ is the signal vector obtained after digital beamforming. The baseband eqvivalent signal vector obtained after digital combiner $\mathbf{W}_{BB}$ is given by

$$\mathbf{y} = \mathbf{W}_{BB}^H\mathbf{r} = \sqrt{\rho}\mathbf{W}_{BB}^H\mathbf{H}_{\text{eff}}\mathbf{t} + \sqrt{\rho}\mathbf{W}_{BB}^H\mathbf{H}_{\text{eff}}\boldsymbol{\Delta}_t \\ + \mathbf{W}_{BB}^H\mathbf{W}_{RF}^H\mathbf{n}. \quad (9)$$

The first term represents the desired signal, the second term is the distortion noise and the third is the Gaussian noise. The covariance matrix of the distortion noise at the transmitter is conditional on the channel realization, and equals $\boldsymbol{\Upsilon}_t = \text{diag}(\mathbf{Q})$, where $\mathbf{Q} = \mathbb{E}\left[\mathbf{t}\mathbf{t}^H\right] = \mathbb{E}\left[\mathbf{F}_{BB}\mathbf{s}\mathbf{s}^H\mathbf{F}_{BB}^H\right] = \frac{1}{N_s}\mathbf{F}_{BB}\mathbf{F}_{BB}^H$. When the columns of $\mathbf{F}_{BB}$ are orthogonal, then $\boldsymbol{\Upsilon}_t = \frac{1}{N_s}\mathbf{F}_{BB}\mathbf{F}_{BB}^H$.

Now, the capacity can be written as

$$R = \mathbb{E}\Bigg\{ \log_2 \Big| \mathbf{I}_{N_s} + R_n^{-1}\mathbf{W}_{BB}^H\mathbf{W}_{RF}^H\mathbf{H}\mathbf{F}_{RF}\mathbf{F}_{BB} \\ \times \mathbf{F}_{BB}^H\mathbf{F}_{RF}^H\mathbf{H}^H\mathbf{W}_{RF}\mathbf{W}_{BB} \Big| \Bigg\}, \quad (10)$$

where

$$R_n = \mathbf{W}_{BB}^H\mathbf{W}_{RF}^H\mathbf{H}\mathbf{F}_{RF}\boldsymbol{\Upsilon}_t\mathbf{F}_{RF}^H\mathbf{H}^H\mathbf{W}_{RF}\mathbf{W}_{BB} + \\ \mathbf{W}_{BB}^H\mathbf{W}_{RF}^H\mathbf{W}_{RF}\mathbf{W}_{BB}\left(\frac{SNR}{N_s}\right)^{-1}. \quad (11)$$

Since finding the closed-form solution of (10) is not straightforward, we provide only Monte Carlo simulations.

B. Analog RF precoding with residual Tx impairments

Let us consider the case $N_{RF} = N_s = 1$ (i.e. analog RF beamforming). From (9), the system model with the distortion noise can be expressed as

$$y = \sqrt{\rho}h_{\text{eff}}s + \delta + n_{\text{eff}}, \quad (12)$$

where $h_{\text{eff}} = \mathbf{w}^H\mathbf{H}\mathbf{f}$ represents the effective channel gain obtained after applying either optimal beamforming and beamcombining vectors or taken from an RF codebook after beamtraining phase, n_{eff} is the effective noise, whereas $\delta \sim \mathcal{CN}\left(\kappa_t^2|\mathbf{w}^H\mathbf{H}\mathbf{f}|^2\rho\right)$ is the transmitter distortion noise. The capacity can be now expressed as

$$R = \mathbb{E}\left\{\log_2\left(1 + \frac{|\mathbf{w}^H\mathbf{H}\mathbf{f}|^2}{|\mathbf{w}^H\mathbf{H}\mathbf{f}|^2\kappa^2 + SNR^{-1}}\right)\right\}. \quad (13)$$

The previous expression can be upper-bounded using Jensen's inequality, i.e. $\mathbb{E}\left[\log_2(1+x)\right] \leq \log_2\left(1 + \mathbb{E}\left[x\right]\right)$ [23], after which we come to

$$R \leq \log_2\left(1 + \mathbb{E}\left\{\frac{|\mathbf{w}^H\mathbf{H}\mathbf{f}|^2}{|\mathbf{w}^H\mathbf{H}\mathbf{f}|^2\kappa^2 + SNR^{-1}}\right\}\right). \quad (14)$$

To solve (14) probability density function (PDF) of the term under expectation is needed. This term can be written $z = \frac{|h_{\text{eff}}|^2}{|h_{\text{eff}}|^2 a + b}$, where $a = \kappa_t^2$ and $b = 1/SNR$. This term, as well the expression in (14), is maximized when the left and right singular vectors corresponding to the largest singular value, $\mathbf{w}$ and $\mathbf{f}$ respectively, are chosen as beamcombining and beamforming vectors. This is an optimal solution (i.e. upper bound).

When the number of antennas at the transmitter N_t and the receiver N_r is large, the left and right singular vectors, $\mathbf{w}$ and $\mathbf{f}$, converge to the array response vectors $\mathbf{a}_r(\theta_l^r, \phi_l^r)$ and $\mathbf{a}_t(\theta_l^t, \phi_l^t)$ respectively, while the singular values converge to $\sqrt{\frac{N_t N_r}{L}}\alpha_l$, $l = 0, ..., L-1$. [6] Therefore, $|h_{\text{eff}}|^2$ converges to $\max_l(\beta_l)$, where $\beta_l = \frac{N_t N_r}{L}|\alpha_l|^2$. β_l is an exponentially distributed random variable (RV) [25] with mean $\overline{\beta_l} = \frac{N_t N_r}{L}\sigma_l^2$. In addition, when N_t and N_r are large, beams become narrow, and once a path with maximal gain is chosen, the contribution from other paths is negligible. When all channel paths are i.i.d. (i.e. there exist L equally probably paths) with the same average power $\overline{\beta_l} = \overline{\beta}$, the cumulative density function (CDF) of the RV $|h_{\text{eff}}|^2$ is given by [17]

$$F_{|h_{\text{eff}}|^2}(z) = F_\beta(z)^L = (1 - e^{-z/\overline{\beta}})^L, \quad (15)$$

while its PDF can be calculated as

$$f_{|h_{\text{eff}}|^2}(z) = \frac{dF_{|h_{\text{eff}}|^2}(z)}{dz} = L\frac{dF_\beta(z)}{dz}F_\beta(z)^{L-1}. \quad (16)$$

Solving the differentiate, (16) can be expressed as

$$f_{|h_{\text{eff}}|^2}(z) = \frac{L}{\overline{\beta}}e^{-z/\overline{\beta}}(1 - e^{-z/\overline{\beta}})^{L-1}. \quad (17)$$

Using the binomial expansion [23], Eq. (17) can be rewritten as

$$f_{|h_{\text{eff}}|^2}(z) = \frac{L}{\overline{\beta}}\sum_{l=0}^{L-1}(-1)^L\binom{L-1}{l}e^{-\frac{l+1}{\overline{\beta}}z}. \quad (18)$$

Now, having the PDF of $|h_{\mathrm{eff}}|^2$, one can express the expectation in (14) as

$$\mathbb{E}\left\{\frac{|h_{\mathrm{eff}}|^2}{|h_{\mathrm{eff}}|^2 a + b}\right\} = \int_0^\infty \frac{|h_{\mathrm{eff}}|^2}{|h_{\mathrm{eff}}|^2 a + b} f_{|h_{\mathrm{eff}}|^2}(z) dz =$$

$$\stackrel{L}{=}\frac{L}{\overline{\beta}} \sum_{l=0}^{L-1} (-1)^L \binom{L-1}{l} \underbrace{\int_0^\infty \frac{|h_{\mathrm{eff}}|^2}{|h_{\mathrm{eff}}|^2 a + b} e^{-\frac{l+1}{\overline{\beta}}z} dz}_{I} \quad (19)$$

With the help of [23, Eq. 3.383.10] and [24, Eq. 5.1.45], the integral I can be evaluated as

$$I = \frac{1}{a} e^{\frac{b}{a}\frac{l+1}{\overline{\beta}}} \frac{\overline{\beta}}{l+1} E_2\left(\frac{b}{a}\frac{l+1}{\overline{\beta}}\right), \quad (20)$$

where $E_2(x) = \int_1^\infty \exp(-xt)dt, \mathcal{R}\{x\} > 0$. Combining (14), (19), and (20), the upper bound of the capacity is derived as

$$R \leq \log_2\left[1 + \sum_{l=0}^{L-1}(-1)^L\binom{L}{l+1}\frac{1}{a}e^{\frac{b}{a}\frac{l+1}{\overline{\beta}}}\frac{\overline{\beta}}{l+1}\right.$$

$$\left. \times E_2\left(\frac{b}{a}\frac{l+1}{\overline{\beta}}\right)\right], a > 0. \quad (21)$$

When $a = \kappa_t = 0$, the upper bound equals to

$$R \leq \log_2\left[1 + \sum_{l=0}^{L-1}(-1)^L\binom{L}{l+1}\frac{\overline{\beta}}{b(l+1)}\right]. \quad (22)$$

IV. NUMERICAL RESULTS

In this section, we present numerical results to evaluate and compare the performance of beamforming mmWave MIMO systems. We consider a hybrid beamforming mmWave MIMO with fully-connected and partially connected structures having $N_{RF} = 4$ RF chains and the same number of data streams, $N_s = 4$. Both transmitter and receiver employ ULA with $N_t = 64$ and $N_r = 16$ antennas, respectively. Nevertheless, extending the analysis for UPA would be straightforward. Distortion due to residual hardware errors is modeled with parameter $\kappa_t \in \{0.1, 0.3, 0.5\}$. We consider a channel with limited number of scatters $L = 5$, such that each scatter has the average power $\sigma_i^2 = 1$. AoDs and AoAs are uniformly distributed over $[-\pi/2, \pi/2]$.

For the hybrid beamforming, we assess the performance in two cases:

(1) entries for the analog RF beamformer/combiner matrix are the array response vectors corresponding to true AoDs/AoAs $(\mathcal{A}_x = [\mathbf{a}_x(\phi_1^x), \mathbf{a}_x(\phi_2^x), ..., \mathbf{a}_x(\phi_L^x)], x \in \{t, r\})$, and

(2) entries for the analog RF beamformer/combiner are taken from the set of array response vectors corresponding to $Q = 5$-bit quantized AoDs/AoAs $(\mathcal{A}_x = [\mathbf{a}_x(\phi_1^x), \mathbf{a}_x(\phi_2^x), ..., \mathbf{a}_x(\phi_{2Q}^x)], x \in \{t, r\})$ with the quantization in u-space $u^x = 2\pi d/\lambda \sin(\phi^x), d = \lambda/2$.

In addition, performance of the system for $N_{RF} = N_s = 1$ corresponding to analog RF beamforming is analyzed.

Fig. 2 plots the capacity of hybrid precoding mmWave MIMO using SS-P in case (1). When the hardware is perfect,
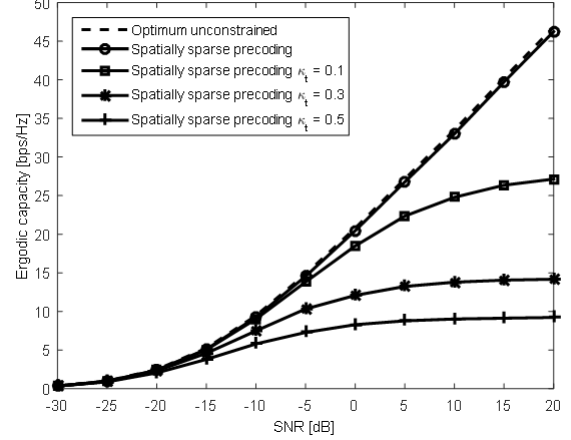

Fig. 2. The capacity of the hybrid precoding mmWave MIMO system with fully-interconnected structure in case (1).
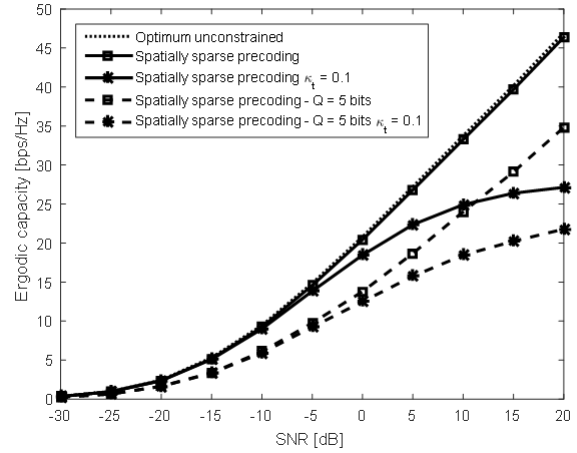

Fig. 3. The capacity of the hybrid precoding mmWave MIMO system with fully-interconnected structure in case (2).

performance of spatially sparse precoding is very close to optimum unconstrained precoding. Under hardware imperfections, its performance is limited by the distortion noise. That is, capacity does not increase with the increase of SNR. Evidently, the performance becomes worse for higher level of the impairments. Fig. 3 compares the capacity of the SS-P under perfect and imperfect hardware ($\kappa_t = 0.1$) in case (1) and case (2). Since in the case (2), the entries for the analog RF precoding matrix are taken from the quantized RF codebook, the performance is lower when compared to the case (1), as expected. The behavior is the same for both ideal and non-ideal hardware scenarios.

The impact of the hardware impairments on the performance of beamforming mmWave MIMO with partially-interconnected RF structure (i.e. using SIC precoding) is depicted in Fig. 4. As for spatially sparse precoding, here the performance is also limited by distortion noise.

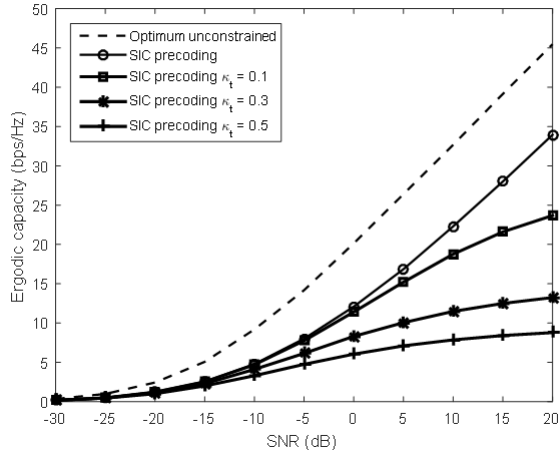Fig. 5 provides the capacity of the analog RF beamforming

Fig. 4. The capacity of the hybrid precoding mmWave MIMO with partially-interconnected structure.
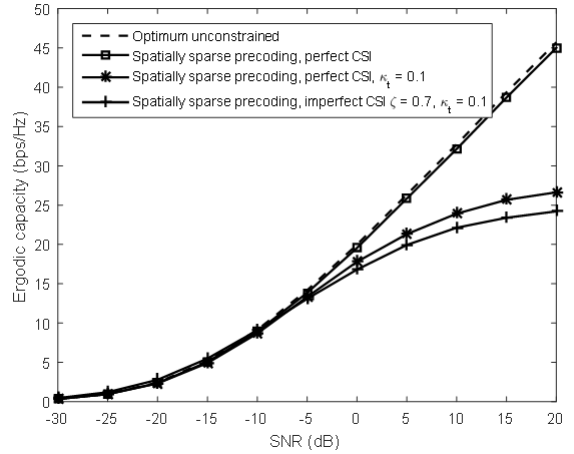

Fig. 6. Impact of aggregated CSI and hardware imperfections on the capacity of hybrid precoding mmWave MIMO system using fully-interconnected structure.
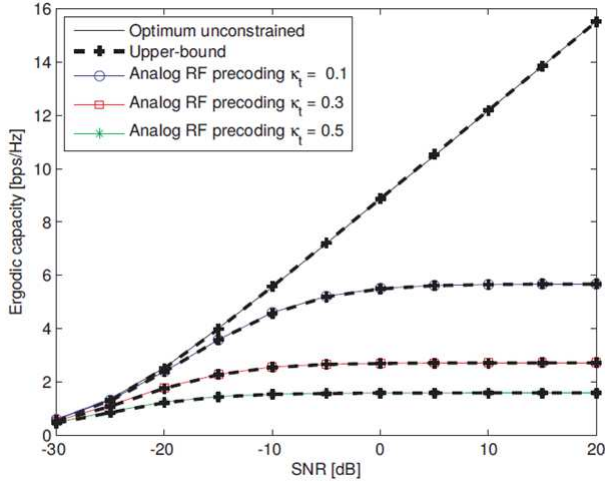

Fig. 5. The capacity of the analog RF precoding mmWave MIMO.
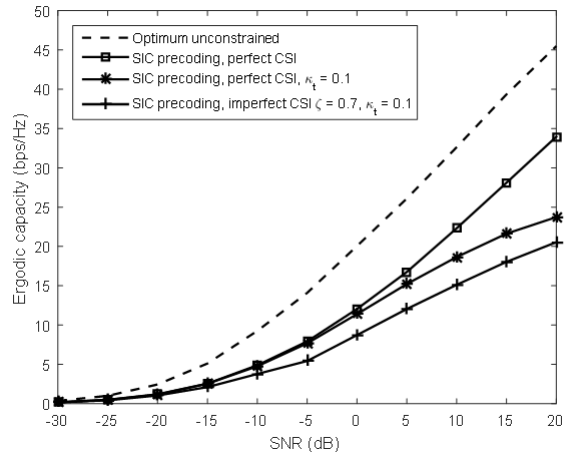

Fig. 7. Impact of aggregated CSI and hardware imperfections on the capacity of hybrid precoding mmWave MIMO system using partially-interconnected structure.

system. Here, only single data stream transmission is possible. Note that in this case too, presence of the distortion noise introduces the effect of ceiling in the performance, meaning that it is not possible to increase the system rate with the higher SNR. In addition to simulation results, analytical upper bound is plotted. Simulation curves are well matched with the upper bound derived in Section III.

Table I compares the achievable rate in ideal and nonideal hardware scenarios, and shows the rate reduction due to hardware impairments for $B = 1.8$ GHz, $SNR = 20$ dB and $\kappa_t = 0.1$.

Finally, we show the performance of both hybrid beamforming mmWave MIMO system using fully-interconnected and partially-interconnected structure under joint CSI imperfections and hardware impairments in Figs. 6 and 7, respectively. We model imperfect channel state information (CSI) as

$$\hat{\mathbf{H}} = \eta\mathbf{H} + \sqrt{1 - \eta^2}\mathbf{E}, \qquad (23)$$

where $\mathbf{H}$ is the actual channel matrix, $\eta \in [0, 1]$ represents the imperfection factor and $\mathbf{E}$ is the error matrix with the i.i.d. entries distributed as $\mathcal{CN}(0, 1)$.

TABLE I
THE RATE REDUCTION DUE TO DISTORTION NOISE.

Rate	SS-P (1)	SS-P (2)	SIC-P	ABF
Perfect HW (Gbps)	82.8	63.0	34.0	28.8
Imperfect HW (Gbps)	50.4	39.6	23.7	10.4
Difference (%)	39.1	37.1	30.3	63.0

V. CONCLUSION

In this paper, we have presented results on the performance of the beamforming mmWave MIMO systems under hardware impairments. The signal model has been extended to include

distortion noise due to imperfect hardware for both hybrid beamforming with fully- and partially-interconnected structure and analog RF beamforming. For the latter, we have also derived the upper bound of the capacity. Numerical results have showed that hardware impairments have significant impact on the system introducing the effect of ceiling in its performance. Future work will extend the analysis to receiver distortion noise as well as to the impact of overall distortion noise on beam search, channel matrix estimation, etc.

REFERENCES

[1] W. Roh, J.-Y. Seol, J. Park, B. Lee, J. Lee, Y. Kim, J. Cho, K. Cheun, and F. Aryanfar, "Millimeter-wave beamforming as an enabling technology for 5G cellular communications: theoretical feasibility and prototype results," *IEEE Commun. Mag.*, vol. 52, no. 2, pp. 106-113, 2014.

[2] T. S. Rappaport, S. Sun, R. Mayzus, H. Zhao, Y. Azar, K. Wang, G. Wong, J. Schulz, M. Samimi, and F. Gutierrez, "Millimeter wave mobile communications for 5G cellular: It will work!," *IEEE Access*, vol. 1, pp. 335-349, 2013.

[3] T. Rappaport, R. W. Heath Jr., T. Daniels, and J. Murdock, *Millimeter wave wireless communications*, Prentice Hall, 2014.

[4] S. Hur, T. Kim, D. Love, J. Krogmeier, T. Thomas, and A. Ghosh, "Millimeter wave beamforming for wireless backhaul and access in small cell networks," *IEEE Trans. Commun.*, vol. 61, no. 10,pp. 4391-4403, 2013.

[5] "Wireless LAN Medium Access Control (MAC) and Physical Layer (PHY) Specifications. Amendment 3: Enhancements for Very High Throughput in the 60 GHz Band," *IEEE Std. 802.11ad*, 2012.

[6] O. E. Ayach, R. W. Heath, S. Abu-Surra, S. Rajagopal and Z. Pi, "The capacity optimality of beam steering in large millimeter wave MIMO systems," *in Proc. 13th International Workshop on Signal Processing Advances in Wireless Communications (SPAWC)*, 2012, pp. 100-104.

[7] J. A. Zhang, X. Huang, V. Dyadyuk and Y. J. Guo, "Massive hybrid antenna array for millimeter-wave cellular communications," *IEEE Wireless Commun.*, vol. 22, no. 1, pp. 79-87, 2015.

[8] S. Han, C. l. I, Z. Xu and C. Rowell, "Large-scale antenna systems with hybrid analog and digital beamforming for millimeter wave 5G," *IEEE Commun. Mag.*, vol. 53, no. 1, pp. 186-194, 2015.

[9] F. Sohrabi and W. Yu, "Hybrid Digital and Analog Beamforming Design for Large-Scale Antenna Arrays," *IEEE J. Sel. Topics Signal Proces.*, vol. 10, no. 3, pp. 501-513, 2016.

[17] M. E. Eltayeb, A. Alkhateeb, R. W. Heath and T. Y. Al-Naffouri, "Opportunistic beam training with hybrid analog/digital codebooks for mmWave systems," *in Proc. Global Conference on Signal and Information Processing (GlobalSIP)*, 2015, pp. 315-319.

[10] F. Sohrabi and W. Yu, "Hybrid beamforming with finite-resolution phase shifters for large-scale MIMO systems," *in Proc. 16th International Workshop on Signal Processing Advances in Wireless Communications (SPAWC)*, 2015, pp. 136-140.

[11] Z. Xu, S. Han, Z. Pan and C. L. I, "Alternating beamforming methods for hybrid analog and digital MIMO transmission," *in Proc. International Conference on Communications (ICC)*, 2015, pp. 1595-1600.

[12] X. Gao, L. Dai, S. Han, C. L. I and R. W. Heath, "Energy-Efficient Hybrid Analog and Digital Precoding for MmWave MIMO Systems With Large Antenna Arrays," *IEEE J. Sel. Areas Commun.*, vol. 34, no. 4, pp. 998-1009, 2016.

[13] O. E. Ayach, S. Rajagopal, S. Abu-Surra, Z. Pi and R. W. Heath, "Spatially Sparse Precoding in Millimeter Wave MIMO Systems," *IEEE Trans. Wireless Commun.*, vol. 13, no. 3, pp. 1499-1513, 2014.

[14] X. Yu, J.-C. Shen, J. Zhang, and K. B. Letaief, "Alternating minimization algorithms for hybrid precoding in millimeter wave MIMO systems," *IEEE J. Sel. Topics Signal Process.*, vol. 10, no. 3, pp. 485-500, 2016.

[15] Y. Li, S. He, C. Ma, S. Ma, C. Li and L. Yang, "Channel Characteristic and Capacity Analysis of Millimeter Wave MIMO Beamforming System," *in Proc. 83rd Vehicular Technology Conference (VTC Spring)*, 2016, pp. 1-5.

[16] S. He, C. Qi, Y. Wu and Y. Huang, "Energy-Efficient Transceiver Design for Hybrid Sub-Array Architecture MIMO Systems," *IEEE Access*, vol. 4, pp. 9895-9905, 2016.

[18] R. Mendez-Rial, C. Rusu, N. Gonzalez-Prelcic, A. Alkhateeb and R. W. Heath, "Hybrid MIMO Architectures for Millimeter Wave Communications: Phase Shifters or Switches?," *IEEE Access*, vol. 4, pp. 247-267, 2016.

[19] T. Schenk, *RF Imperfections in High-Rate Wireless Systems: Impact and Digital Compensation*, Springer, 2008.

[20] X. Zhang, M.Matthaiou, E. Bjornson and M. Coldrey, "Impact of residual transmit RF impairments on training-based MIMO systems," *IEEE Trans. Commun.*, vol. 63, no. 8, pp. 2899-2911, 2015.

[21] J. Zhang, L. Dai, X. Zhang, E. Bjornson and Z. Wang, Achievable Rate of Rician Large-Scale MIMO Channels with Transceiver Hardware Impairments, *IEEE Trans. Veh. Technol.*, vol. 65, no. 10, pp. 8800-8806, 2016.

[22] E. Bjornson, M. Matthaiou and M. Debbah, "A New Look at Dual-Hop Relaying: Performance Limits with Hardware Impairments," *IEEE Trans. Commun.*, vol. 61, no. 11, pp. 4512-4525, 2013.

[23] I. S. Gradshteyn and I. M. Ryzhik, *Tables of Integrals, Series and Products*, 7th Ed., Elsevier, 2007.

[24] M. Abramowitz and I. A. Stegun, *Handbook of Mathematical Functions*, New York: Dover, 1974.

[25] A. Papoulis and S. U. Pillai, *Probabilities, Random Variables and Stochastic Processes*, 4th Edition, McGraw-Hill Europe, 2002.